Facilitation of Early and Middle Latency SEP after tDCS of M1

No Evidence of Primary Somatosensory Homeostatic Plasticity

Zolezzi, Daniela M; Larsen, Dennis B; Zamorano, Anna M; Graven-Nielsen, Thomas

Published in:
Neuroscience

DOI (link to publication from Publisher):
10.1016/j.neuroscience.2024.05.001

Publication date:
2024

Document Version
Publisher's PDF, also known as Version of record

Neuroscience 551 (2024) 143–152

Contents lists available at ScienceDirect

Neuroscience

journal homepage: www.elsevier.com/locate/nsc

Research Article

Facilitation of Early and Middle Latency SEP after tDCS of M1: No Evidence of Primary Somatosensory Homeostatic Plasticity

Daniela M. Zolezzi, Dennis B. Larsen, Anna M. Zamorano, Thomas Graven-Nielsen *

Center for Neuroplasticity and Pain (CNAP), Department of Health Science and Technology, Aalborg University, Aalborg, Denmark

ARTICLE INFO

Key words:
somatosensory evoked potentials
homeostatic plasticity
primary motor cortex
primary sensory cortex
transcranial direct current stimulation

ABSTRACT

Homeostatic plasticity is a mechanism that stabilizes cortical excitability within a physiological range. Most homeostatic plasticity protocols have primed and tested the homeostatic response of the primary motor cortex (M1). This study investigated if a homeostatic response could be recorded from the primary sensory cortex (S1) after inducing homeostatic plasticity in M1. In 31 healthy participants, homeostatic plasticity was induced over M1 with a priming and testing block of transcranial direct current stimulation (tDCS) in two different sessions (anodal and cathodal). S1 excitability was assessed by early (N20, P25) and middle-latency (N33-P45) somatosensory evoked potentials (SEP) extracted from 4 electrodes (CP5, CP3, P5, P3). Baseline and post-measures (post-priming, 0-min, 10-min, and 20-min after homeostatic induction) were taken. Anodal M1 homeostatic plasticity induction significantly facilitated the N20-P25, P45 peak, and N33-P45 early SEP components up to 20-min post-induction, without any indication of a homeostatic response (i.e., reduced SEP). Cathodal homeostatic induction did not induce any significant effect on early or middle latency SEPs. M1 homeostatic plasticity induction by anodal stimulation protocol to the primary motor cortex did not induce a homeostatic response in SEPs.

Introduction

Synaptic plasticity is a ubiquitous mechanism that allows the nervous system to adapt in an experience-dependent manner. Due to its feedforward nature, a balance between excitation and inhibition becomes crucial if excess neuronal excitability is to be prevented (Turrigiano and Nelson, 2004). Homeostatic plasticity balances net cortical excitability by shifting the threshold for inducing long-term potentiation (LTP) or depression (LTD) based on the preceding state of excitability (Bienenstock et al., 1982; G, 2011; Turrigiano, 2012). This mechanism can be induced in humans using non-invasive brain stimulation (NIBS) such as repetitive transcranial magnetic stimulation (TMS) and transcranial direct current stimulation (tDCS) (Wittkopf et al., 2021a). In healthy subjects, a single block (i.e., priming) of excitatory NIBS to the primary motor cortex increases net cortical excitability, which is thought to reflect the synaptic relays within the corticomotor pathway (i.e., LTP-like) (Siebner and Rothwell, 2003; Ziemann et al., 2008). If another block of excitatory NIBS is delivered, separated by 10 mins or less of non-stimulation, a homeostatic response can be shown as reflected by decreased net corticomotor excitability (i.e., LTD-like) that lasts up to 30 mins post protocol (Karabanov et al., 2015; Wittkopf et al., 2021b). To date, most homeostatic plasticity protocols have primed and tested the hand area of the primary motor cortex (M1) and inferred homeostatic responses based on TMS motor evoked potentials (MEP) (Karabanov et al., 2015; Thapa and Schabrun, 2018; Wittkopf et al., 2021b). Prolonged experimental pain is known to impair corticomotor homeostatic plasticity (Thapa et al., 2021; Wittkopf et al., 2023) and affect early- and middle-latency somatosensory evoked potentials (SEP) (De Martino et al., 2018) and yet it is still unknown if these somatosensory excitability

Abbreviations: M1, Primary Motor Cortex; S1, Primary Sensory Cortex; tDCS, Transcrnaial Direct Current Stimulation; SEP, Somatosensory Evoked Potential; LTP, Long-term Potentiation; LTD, Long-term Depression; NIBS, Non-invasive Brain Stimulation; TMS, Repetitive Transcranial Magnetic Stimulation; STAI, Spielberger State-Trait Anxiety Inventory; BDI-II, Becks Depression Inventory-II; PSQI, Pittsburg Sleeping Questionnaire Inventory; TASS, Transcranial Magnetic Stimulation Adult Safety Screen; EEG, Electroencephalogram; MRI, Magnetic resonance imaging; ICA, Independent Component Analysis; SMC, Sensorimotor Cortex; MEP, Motor Evoked Potential; HFOs, High Frequency Oscillations; tACS, Transcranial Alternating Current Stimulation.

* Corresponding author. Address: Center for Neuroplasticity and Pain (CNAP) Department of Health Science and Technology Faculty of Medicine, Aalborg University Selma Lagerløfs Vej 249, 9260 Gistrup, Denmark.

E-mail address: tgn@hst.aau.dk (T. Graven-Nielsen).

https://doi.org/10.1016/j.neuroscience.2024.05.001
Received 22 December 2023; Accepted 1 May 2024
Available online 11 May 2024

changes are related to impaired corticomotor homeostatic plasticity. Additionally, chronic pain patients (e.g., migraine and chronic low back pain) have shown an impaired homeostatic response (Quartarone et al., 2005; Thapa et al., 2021), which is hypothesized to contribute to disproportionately high synaptic strengthening, increased pain perception, aberrant cortical reorganization, and sensorimotor dysfunction (Kang et al., 2011; Thapa et al., 2018, 2021).

Only two studies have explored the primary somatosensory (S1) excitability after somatosensory homeostatic plasticity protocols (Bliem et al., 2008; Jones et al., 2016), with inconclusive results. Exploring S1 excitability after inducing corticomotor homeostatic plasticity, may offer an approach to elucidate the known concurrent S1 and M1 excitability changes that happen during pain (Schabrun et al., 2013; Vaseghi et al., 2015a; Wittkopf et al., 2023). If cortical homeostatic plasticity is a global mechanism, then it is plausible that M1-S1 connections, which have been studied in human and animal models (Jones et al., 1978; Rocco-Donovan et al., 2011; Frot et al., 2013), drive the homeostatic regulation of S1. In addition, considering that tDCS is diffuse (Opitz et al., 2015), S1 could also be directly modulated by modulating M1. To study S1-specific excitability changes, the current study will focus on the earliest SEP cortical complex (~20 ms after stimulation, N20-P25) which originates from S1 in area 3b of the post-central gyrus (Brodmann's areas 3b) (Bradley et al., 2016; Rezaei et al., 2021), and the middle-latency SEP, N33-P45, generated within S1 in areas 1 and 2 at the crown of the sulcus (Allison et al., 1991; Inui et al., 2004; Bradley et al., 2016).

Using a protocol that has shown excellent test–retest reliability for homeostatic plasticity induction over M1 (Wittkopf et al., 2021b), this study aimed to evaluate the somatosensory response of S1 to homeostatic plasticity induction over M1. Thus, it was hypothesized that the early- and middle-latency SEP components (N20-P25 and N33-P45) would exhibit a homeostatic plasticity response by a reversal of SEP excitability after the homeostatic plasticity protocol.

Experimental procedures

Participants

Thirty-one healthy individuals (age: 27.0 ± 3.5, 12 females) participated in the experiment (Detailed inclusion/exclusion criteria in Supplementary Material) and gave written informed consent. Two subjects had to be excluded due to data quality purposes, thus 29 subjects were included in the final analyses. Psychological and lifestyle factors were evaluated based on (1) Spielberger State-Trait Anxiety Inventory (STAI), (2) Becks Depression Inventory-II (BDI-II), and (3) Pittsburg Sleeping Questionnaire Inventory (PSQI). The demographic characteristics of the subjects are summarized in Table 1 (see also Supplementary Material, for a detailed description of the questionnaires).

Additionally, subjects needed to confirm not being in any type of acute pain at the time of the experiment. Prior to the start of the experiment, subjects completed the Transcranial Magnetic Stimulation Adult Safety Screen (TASS) (Keel et al., 2001), which ensures safety for tDCS stimulation as well (Poreisz et al., 2007). This study was approved by the Ethics Committee for the North Denmark Region (VN-20210047) and performed according to the Helsinki Declaration.

Experimental design

The study was a randomized cross-over study comprising two sessions separated by at least 1-week apart to control for carryover effects, in which only the type of tDCS stimulation for the priming and testing blocks varied (i.e., anodal-anodal or cathodal-cathodal). Participants sat in a comfortable chair and were instructed to sit relaxed with their eyes open looking at the center of a cross 60 cm away while the EEG was recorded and the electrical stimuli were delivered. In each session, electrically evoked SEPs were recorded at five different time points to assess S1 cortical excitability before and after the induction of M1 homeostatic plasticity (Fig. 1): Baseline (i.e., before priming block), post-priming block (Post-Priming), immediately post homeostatic induction (Post-HP), 10 min post homeostatic induction (Post + 10 min), and 20 min post homeostatic induction (Post + 20 min).

Table 1
Descriptive and demographic characteristics of the study sample

	N = 29[1]	Questionnaire scores[2]
Age	27.17 (3.34)	
Sex		
M	18/29 (62%)	
F	11/29 (38%)	
Weigth	68.13 (11.52)	
Heigth	174.09 (7.57)	
Handness		
Right	25/29 (86%)	
Left	4/29 (14%)	
BDI		9 (9)
Normal	18/28 (64%)	
Mild	4/28 (14%)	
Moderate	2/28 (7.1%)	
Severe	4/28 (14%)	
S-Anxiety		34 (19)
Low	19/29 (66%)	
Moderate	9/29 (31%)	
High	1/29 (3.4%)	
T-Anxiety		38 (22)
Low	16/29 (55%)	
Moderate	13/29 (45%)	
PSQI		5 (3)
Good (PSQI ≤ 5)	19/29 (65%)	
Poor (PSQI ≥ 5)	10/29 (35%)	

[1] Mean (SD); n/N (%).
[2] Median (IQR), score calculation and details can be found in Supplementary Material.

Electrical stimulation

A constant current stimulator (NoxiTest IES 230, Noxitest, Aalborg, Denmark) was used to deliver electrical stimuli to the right median nerve and controlled by LabVIEW (Aalborg University, Aalborg, Denmark). Each time point included one block of 500 monophasic square-wave electrical pulses of 0.2 ms duration (Cruccu et al., 2008). The stimulation rate was 2 Hz (Bliem et al., 2008; Bradley et al., 2016) and had a 20% variance to avoid accommodation. The stimulation electrodes in use were 15 mm x 20 mm Ag-AgCL electrodes (Neuroline 700; Ambu, Ballerup, Denmark). The anode was placed at the wrist crease and the cathode 2 cm proximally (Fig. 1). The perception threshold was detected individually by the method of limits. The stimulus intensity was then obtained three times the perception threshold (Cruccu et al., 2008), and all participants confirmed a clear but non-painful electrical sensation. The mean intensity for stimulation for all subjects was 5.41 ± 1.77 mA and 5.16 ± 1.70 m A, for the first and second session, respectively.

Homeostatic plasticity protocol

Homeostatic plasticity was induced in the left M1 by applying tDCS for 7 min (priming block), followed by 5 min of no stimulation and then a testing block of tDCS lasting 5 min (Fig. 1). These stimulation periods for priming, resting (no-stimulation), and testing have reliably elicited homeostatic plasticity in M1 at 10 min post-testing block (Wittkopf et al., 2021a, 2021c). A constant current of 1 mA was delivered through a tDCS system (Starstim 32, Neuroelectrics, Barcelona, Spain) using two 12 mm diameter sintered Ag/AgCl pellet gel elec-

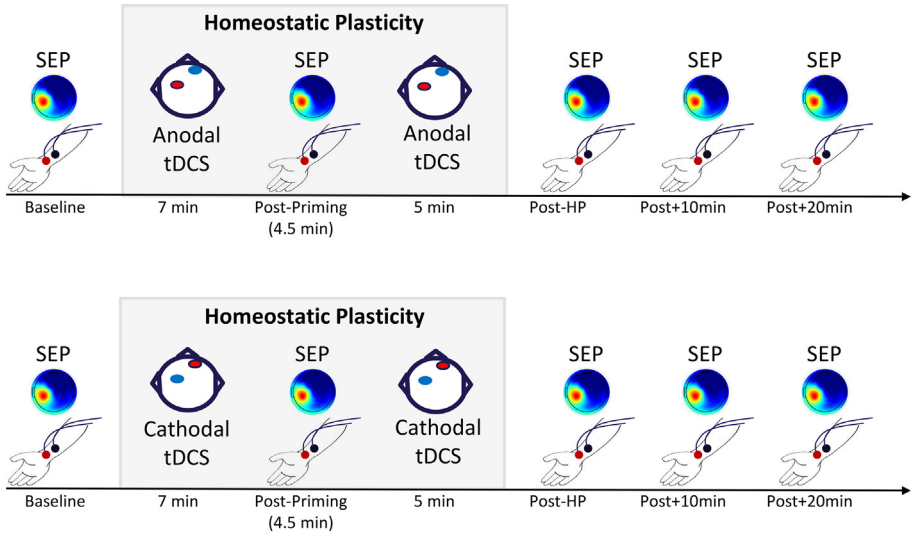

Fig. 1. Experimental design for evaluating S1 excitability after the M1 homeostatic plasticity induction protocol. Two randomized cross-over sessions were separated by at least 1-week, where the polarity of transcranial direct current stimulation (tDCS) in the homeostatic plasticity induction varied. The homeostatic plasticity protocol consisted of two blocks of tDCS: priming (7 min), rest (5 min), and a testing block (5 min). S1 excitability was assessed through SEPs recorded at five time points: baseline, post-priming (during the homeostatic plasticity rest, Post-Priming), immediately (Post-HP), 10 min (Post + 10 min), and 20 min (Post + 20 min) post homeostatic plasticity induction.

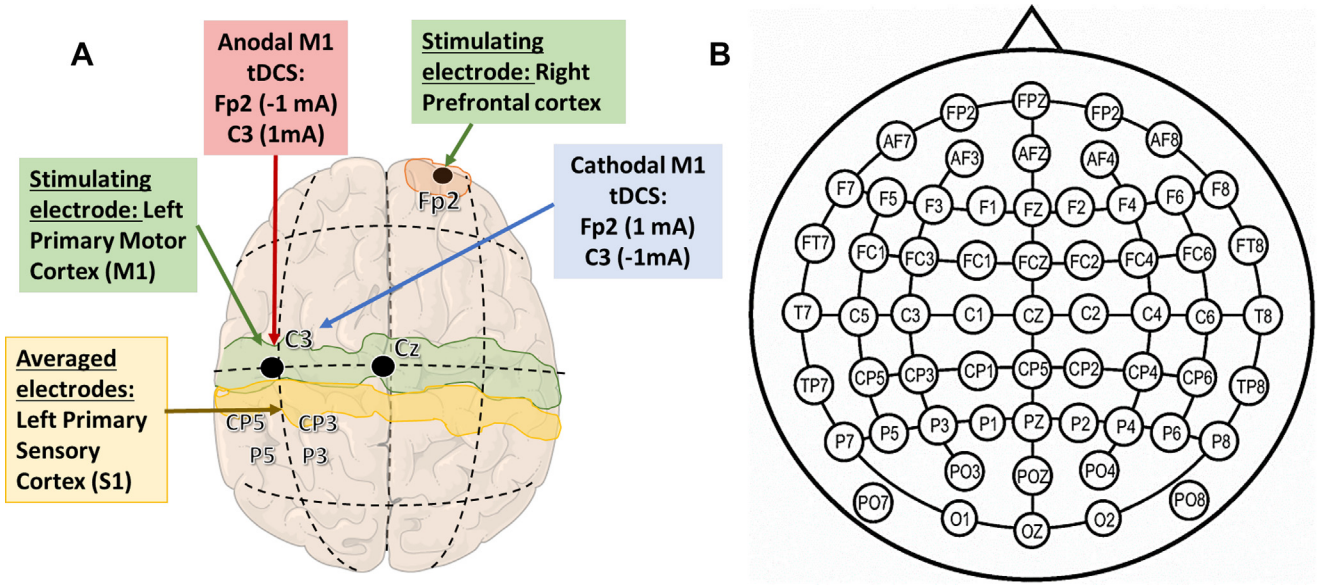

Fig. 2. Layouts for homeostatic plasticity **induction and EEG recording. A.** Electrode positions for M1 homeostatic induction protocol according to anodal or cathodal transcranial direct current stimulation (tDCS). The four electrodes (CP5, CP3, P5 and P3) which were averaged posterior of C3 are also demonstrated. **B.** Topographical map for the 64 EEG channel cap according to the 10/20 system (two channels correspond to earlobe references and are not depicted).

trodes placed according to the 10/20 electroencephalogram (EEG) system. In one session, anodal tDCS was applied at C3 (anode, 1 mA) and FP2 (cathode, −1 mA, Fig. 2A). Conversely, in the other session, cathodal tDCS was applied at C3 (cathode, −1 mA) and FP2 (anode, 1 mA, Fig. 2A). Subjects were told that the stimulation could be felt as itching, slight burning, tingling, or prickling sensation that would peak at 30 s and progressively decrease after 1 min approximately.

Transcranial direct current stimulation electrical field modeling

Electrical field modeling was used to determine the extent of stimulation of the tDCS current, and whether the C3 electrode also directly stimulated S1 (Opitz et al., 2015), given the use of a standard contralateral two-electrode montage. The electric field modeling was done through SimNIBS 4 (https://www.simnibs.org, Copenhagen, Denmark) (Saturnino et al., 2019), an open-source software package for the simulation of NIBS. The simulation was done through MATLAB scripting where the specific size (6 mm radius) and shape (circular) of the tDCS electrodes were configured. The magnetic resonance imaging (MRI) head model (SimNIBS "m2m_ernie") was used for anatomical estimation, as individual brain anatomy of the subjects was not obtained. A simple ROI analysis was done to estimate the mean electrical magnitude for S1 and M1 according to the three-dimensional coordinates defined previously (Mayka et al., 2006).

Encephalographic recording and preprocessing

Somatosensory-evoked potentials were recorded at 2400 Hz without filter settings (g.HIamp biosignal amplifier g.Tec medical engineering GmbH, Schiedlberg, Austria) and a 64-channel encephalographic electrode cap (gTEC.hiAMP) according to the 10–20 international system (Fig. 2B). Only 62 EEG channels were recorded as two were used for stimulation (C3 and FP2). Electrode impedances were kept below 10 kΩ.

EEGLAB (v2021.0) and MATLAB (2021b) were used to preprocess and analyze data offline. First, channel baselines were removed after which the data was referenced to the right earlobe ipsilateral to the stimulated hand (Tomberg et al., 1991), band-pass filtered (0.3–100 Hz, with an 8th order Butterworth filter) and notch filtered for line noise removal (50 Hz, 4th order Butterworth filter). Transient and large amplitude artifacts were removed using an artifact subspace reconstruction threshold value of $k = 30$ (CleanRawData) (Chang et al., 2020). Subsequently, the referenced EEG dataset (before filtering) was duplicated, and EEG signals were high pass filtered at 1 Hz (8th order Butterworth filter) for independent component analysis (ICA). ICA components (ocular, muscular, cardiac, and channel artifacts) were detected using the ICLabel EEGLAB plugin (Pion-Tonachini et al., 2019). Then, the ICA weights were transferred to the original filtered data set (0.3–100 Hz), and ICA components were examined visually and removed manually. EEG data was then segmented into 300 ms epochs (from −100 ms to 200 ms) and baseline correction was performed for each epoch (−100 to −10 ms) before averaging across epochs.

Somatosensory-evoked potentials

After constructing a grand-average SEP across epochs and subjects (Fig. 3). The SEP components (N20, P25, N33, P45) were defined as the most negative or positive peaks within a specific time window after stimulation, in which the latencies of each peak were extracted. For N20, it was 17–21 ms (Bliem et al., 2008; Bradley et al., 2016), 23–31 ms for P25, 28–35 ms for N33 (i.e., parietal component of the N30 frontal component), and 38–50 ms for P45 (Bradley et al., 2016). For each time point, a pool of four parietal and centro-parietal electrodes (CP3, CP5, P3, and P5) was selected and their signals averaged to create a region of interest where the components showed the highest amplitude. Besides the single SEP peaks, the N20-P25 and N33-P45 peak-to-peak complexes were also calculated and analyzed. N20-P25 was calculated from the difference between P25 and N20. N33-P45 complex was computed from the difference between P45 and N33. Two subjects were deleted from all analyses for not displaying a SEP response to electrical stimulation. Additionally, subjects who had baseline values below 0.1 μV (for a certain peak or component) were also deleted from that analysis. Thus, for each peak and complex, the following subjects were analyzed: for N20 and N20-P25, 27 subjects; for P25 and N33, 25 subjects; for P45, 26 subjects; and for N33-P45, 27 subjects.

Statistical analysis

Following data inspection, the amplitude of SEP peaks and complexes was normalized to baseline values for each time point in each session. The latencies of N20, P25, N33 and P45 were analyzed in their raw state (ms after stimulation). Before statistical analysis, assumptions of normality were tested Shapiro Wilk's test for normality. Levene's test, and Boxes M test, were used for homogeneity of variances, and homogeneity of covariances respectively. The normalized SEP values were analyzed in a two-way repeated measure analysis of variance (ANOVA) with time (Baseline, Post-Priming, Post-HP, Post + 10 min, Post + 20 min) and tDCS type (Anodal or Cathodal)

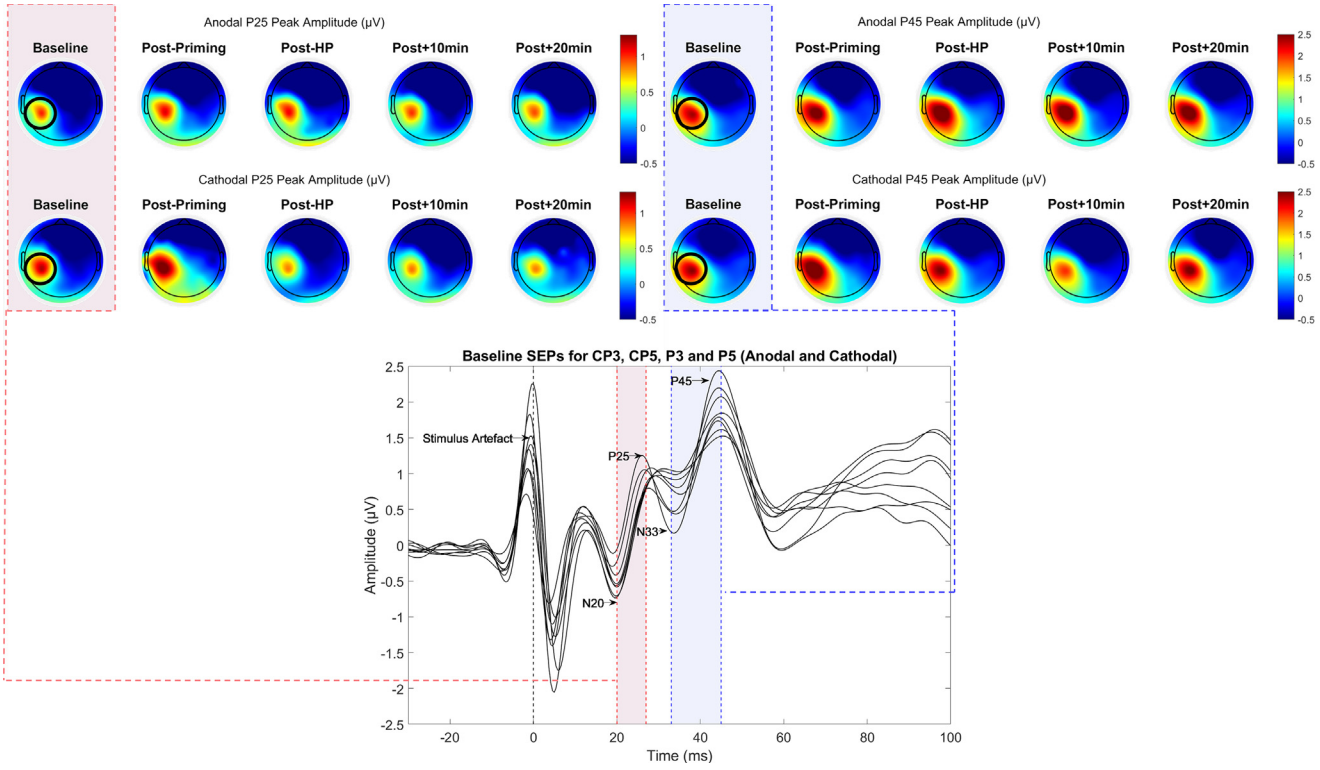

Fig. 3. Topographical maps for P25 and P45 at every time point for both sessions. The topoplots show the evoked potentials for each session at every time point of analysis for the 62 EEG channels. The amplitude of the topoplots is represented at 25 ms (left) and 45 ms (right). In the baseline topoplots, the black circle highlights the electrodes that were averaged as a region of interest (CP3, P3, CP5, and P5). At the bottom, the SEP traces correspond to the grand-average baselines of these electrodes for both sessions, identifying the peaks of activity. N20-P25 interval in red. N33-P45 interval in blue. (For interpretation of the references to colour in this figure legend, the reader is referred to the web version of this article.)

as factors. Greenhouse-Geisser correction was applied if the sphericity assumption was violated. In the case of a significant two-way interaction, multiple pairwise comparisons were conducted with False Discovery Rate (FDR) correction for multiple comparisons, over the effect of tDCS type at every timepoint and the effect of time at each level of tDCS type. Significance was accepted for $p < 0.05$. All computations for the statistical analysis were performed in RStudio (1.2.5033).

Results

Safety and side effects

Most of the subjects experienced a slight local tingling or itching under the tDCS electrodes. Only two subjects reported these sensations as painful, which ceased the first 10–20 s of the experiment. Thus, the experimental procedures were not interrupted by any adverse effects. No participant reported any side effects after the stimulation ended.

Electric field modeling

The electric field modeling over C3 for anodal and cathodal tDCS indicates modulation of both the precentral and postcentral gyrus (Fig. 4), with a higher magnitude of electrical current reaching M1 than S1 (Table 2). The regions where M1 and S1 overlap exhibit a lower magnitude of the electrical field than the one over M1 directly. Thus, it can be inferred that S1 was stimulated by the M1 homeostatic plasticity protocol, but the magnitude of current differed from that in M1.

Early latency somatosensory evoked potentials

The N20 peak ratio of anodal and cathodal stimulation were different (Fig. 5A) as indicated by a significant ANOVA effect of tDCS type, but there was no significant interaction or time effect (Table 3).

The P25 peak amplitude (Fig. 5B) showed a significant interaction, a main effect of tDCS type, and no significance for time (Table 3). Within the anodal tDCS, the P25 peak ratio increased between Post-Priming and Post-HP ($p = 0.004$), Post-Priming and Post + 10 min ($p = 0.0008$), and Post-Priming and Post + 20 min ($p = 0.007$). Conversely, within the cathodal tDCS, the P25 peak ratio did not change over time. Moreover, anodal tDCS elicited an increase in the P25 peak ratio when compared to cathodal tDCS, at Post + 10 min ($p = 0.014$) and Post + 20 min ($p = 0.006$).

For the N20-P25 complex (Fig. 5C) a significant interaction was found, with significant main effects of time and tDCS type (Table 3). An increase in the N20-P25 complex within the anodal tDCS between Post-Priming and Post-HP ($p < 0.0001$), Post-Priming and Post + 10 min ($p < 0.0001$), and Post-Priming to Post + 20 min ($p < 0.0001$). For cathodal tDCS, a decrease in the N20-P25 ratio was found between Post-HP and Post + 10 min, ($p = 0.015$). Additionally, anodal tDCS increased the N20-P25 ratio when compared to cathodal tDCS at Post-HP ($p = 0.006$), Post + 10 min ($p < 0.0001$) and Post + 20 min ($p = 0.016$). There were no differences in the latencies of N20 and P25 ($p > 0.05$) (Supplementary Material).

Early to middle latency somatosensory evoked potentials

The N33 peak ratios had no significant interaction, while a significant main effect of tDCS type was found with higher overall N33 peak ratios for anodal tDCS (Fig. 6A and Table 4).

The P45 peak ratio (Fig. 6B) showed a significant interaction effect and main effect of time (Table 4). The P45 peak ratio increased across time within anodal tDCS from Post-Priming to Post-HP ($p < 0.0001$), Post + 10 min ($p < 0.0001$), and Post + 20 min ($p < 0.0001$). There were no significant differences over time within cathodal tDCS. In addition, anodal tDCS was different from cathodal tDCS at Post-HP ($p = 0.002$), Post + 10 min ($p < 0.0001$), and Post + 20 min ($p = 0.0001$).

The N33-P45 complex (Fig. 6C) indicated a significant interaction, main effect of time and tDCS type (Table 4). Within anodal tDCS, the N33-P45 complex increased compared to Post-Priming at Post-HP ($p < 0.0001$), Post + 10 min ($p < 0.0001$), and Post + 20 min ($p < 0.0001$), while cathodal tDCS did not elicit any significant effects on the N33-P45 complex ratio over time. Moreover, the type of tDCS affected the N33-P45 complex ratio, with higher ratios for anodal tDCS compared to cathodal tDCS at Post-HP ($p = 0.002$), Post + 10 min ($p < 0.0001$) and Post + 20 min ($p = 0.0001$). There were no differences in the latencies of N33 or P45 ($p > 0.05$) (Supplementary Material).

Discussion

The present study aimed to evaluate if homeostatic plasticity induced at M1 regulates S1 excitability as reflected by early- and middle-latency SEPs. These results suggest that M1 homeostatic plasticity induction did not induce a homeostatic response as evaluated by SEPs.

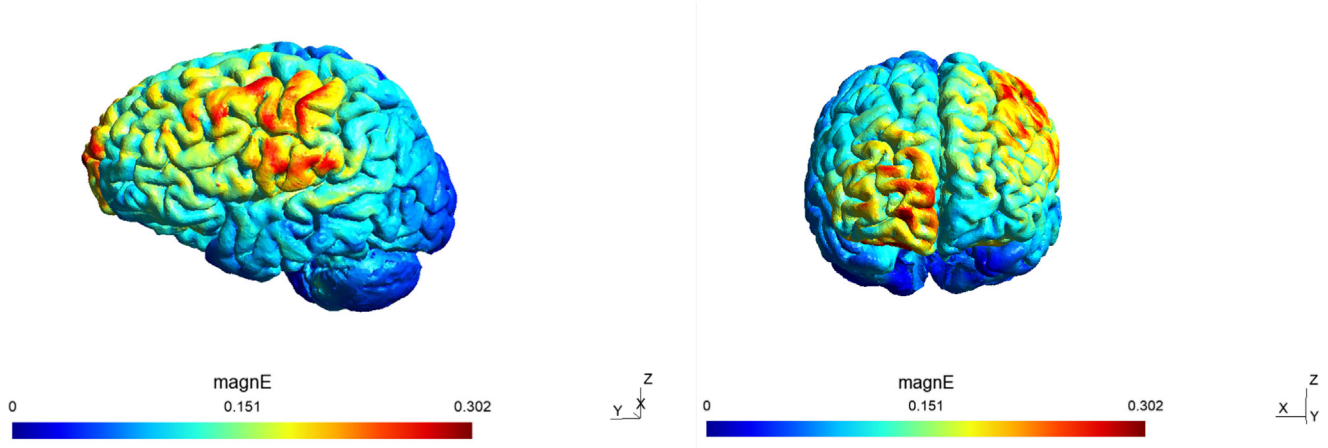

Fig. 4. Electrical Modeling for tDCS. Lateral and frontal view of the electric field magnitude (magnE) generated in SimNIBS for tDCS over M1. The graphs describe magnitude rather than polarity, thus representing both anodal and cathodal tDCS.

Table 2
Mean electrical field magnitude according to three-dimensional locations for M1 and S1

ROI	$PEAK_X$	$PEAK_Y$	$PEAK_Z$	MEAN magnE
M1	−37	−21	54	0.158062
S1	−40	−24	50	0.118974
SENSORIMOTOR CORTEX (SMC)[1]	−39	−21	54	0.159198
S1 AND M1 OVERLAPPING REGIONS	−41	22	49	0.110651

Coordinates were taken from (Mayka et al., 2006). The mean electrical field magnitude in each ROI was calculated using a standard mesh head (SimNIBS) and the size of the electrodes in this study.
[1] SMC is divided into M1 (Brodmans area 4) and S1 (Brodmans area 1,2,3).

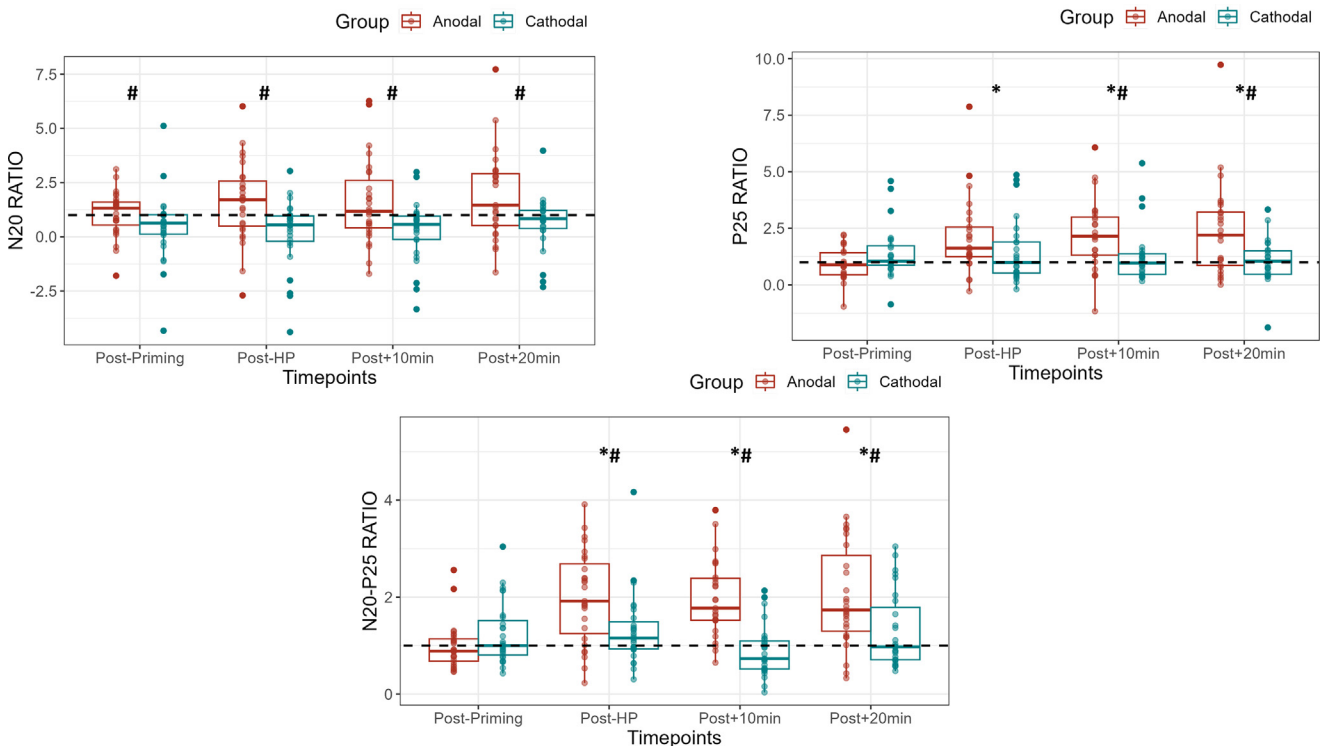

Fig. 5. Box and whiskers plot for N20, P25, and N20-P25 somatosensory evoked potentials normalized to baseline following induction of homeostatic plasticity by anodal and cathodal tDCS. The box representing the median and 25th and 75th quartiles and the "whisker" showing the 5th and 95th percentile. Significant difference in SEP components within time for type of tDCS compared to Post-Priming ($^{*}p < 0.05$). Significant difference between anodal and cathodal stimulation ($^{\#}p < 0.05$).

Table 3
Main and interaction effects for the two-way repeated measures ANOVA in N20, P25, and N20-P25

	TIME	GROUP	TIME:Group
N20			
F	1.347	21.623	1.454
P	0.269	0.000084*	0.234
P25			
F	2.24	5.55	6.93
P	0.091	0.027*	0.00036*
N20-P25			
F	12.374	10.582	13.371
P	0.000001*	0.003*	0.000000398*

Early latency sensory evoked potentials as S1 cortical excitability measures

To evaluate changes in S1 excitability after the M1 homeostatic plasticity induction protocol, early SEP peaks and complexes were investigated. It has been robustly reported that non-noxious electrical stimulation triggers hierarchical processing proceeding from the thalamus to S1 (parietal cortex) and after some tens of milliseconds to S2 (parietal operculum) (Allison et al., 1989b, 1989a, 1991; Inui et al., 2004). N20 has been an indicator of the integrity of S1 (Desmedt et al., 1987), where area 3b ablations have impaired all types of tactile sensation from the lemniscal pathway (Knecht et al., 1996), and deactivated the corresponding associative parts of area 1 (Garraghty et al., 1990). Moreover, lesions in area 1 and 2 impair higher-order tasks such as discrimination of textures (Randolph and Semmes, 1974; Garraghty et al., 1990). These findings support that N20-P25 (area SI-3b), and N33-P45 (area SI-1/2), indicate an excitability change from S1 (Allison et al., 1989b, 1989a, 1991; Matsunaga et al., 2004; Valeriani et al., 2004; Frot et al., 2013; Bradley et al., 2016). The present study found facilitation of N20-P25, P45, and N33-P45 early SEP components, confirming an excitability change at S1 after an anodal M1 homeostatic plasticity induction protocol and revealing a different tDCS effect depending on the evaluated SEP component and modality of tDCS. For instance, the lack of effect for the N20 peak seen in this study follows the findings of previous studies after NIBS (Enomoto et al., 2001; Matsunaga et al., 2004; Bliem et al., 2008). N20 is a more

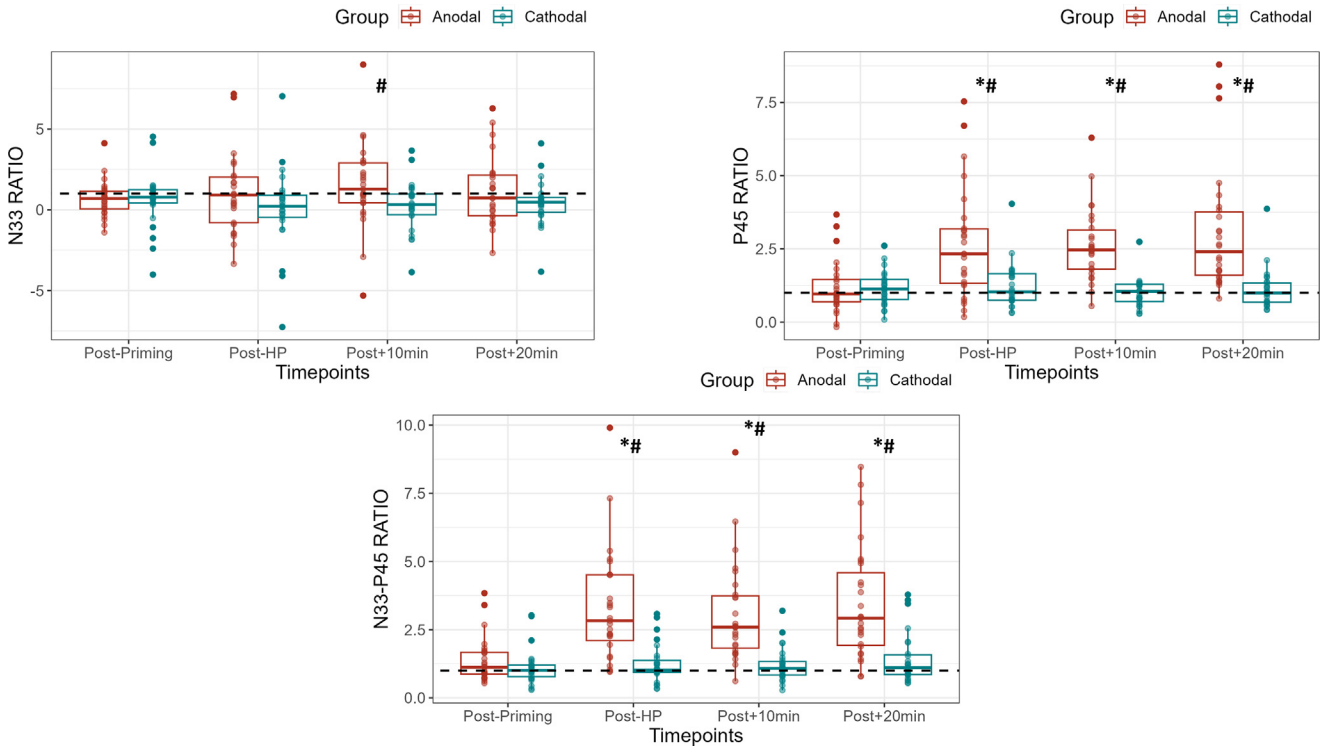

Fig. 6. Box and whisker plot for N33, P45, and N33-P45 somatosensory evoked potentials normalized to baseline following induction of homeostatic plasticity by anodal and cathodal tDCS. The box representing the median and 25th and 75th quartiles and the "whisker" showing the 5th and 95th percentile. *Significant difference in SEP ratio within time for type of tDCS compared to Post-Priming. #Significant difference between anodal and cathodal stimulation. Significance: $^{*}p < 0.05$; $^{\#}p < 0.05$.

Table 4
Main and interaction effects for the two-way repeated measures ANOVA in N33, P45 and N33-P45 complex

	TIME	GROUP	TIME:Group
N33			
F	0.430	4.845	1.432
P	0.732	0.038*	0.241
P45			
F	12.855	17.768	16.644
P	0.000000729*	0.000285*	0.000000022*
N33-P45			
F	14.316	28.208	14.373
P	0.000000161*	0.0000148*	0.000000153*

subcortical component of pyramidal cells in layer 4 from S1 (Allison et al., 1991), thus unlikely to be significantly polarized by tDCS (Matsunaga et al., 2004). Another evidence that supports the hypothesis of spatially restricted effects to subcortical components (Nitsche and Paulus, 2000) is the lack of tDCS effect on high frequency oscillations (HFOs) (Hashimoto et al., 1996), a component of SEPs originating subcortically (i.e., thalamus, thalamocortical afferents or post-synaptic activities) (Dieckhöfer et al., 2006). Additionally, there was no change of HFOs after transcranial alternating current stimulation (tACS) (Fabbrini et al., 2022) until tACS was synchronized to individual HFOs, supporting their thalamocortical origin and suggesting a plausible way to modulate thalamocortical activity (Cruciani et al., 2024). Adding to the previous knowledge, N20 revealed a significant difference between the type of tDCS in the present study. P25 reflects a more superficial portion of apical dendrites located in layers 2/3 of area 3b (Allison et al., 1991) and is more likely to be polarized by the tDCS. The tDCS effect is notably increased for N33-P45, which could reflect the distinct processing functions of somatosensory areas within SI (area 3b versus areas 1–2) (Bradley et al., 2016). From an evolutionary perspective, area 1–2 from S1 (N33-P45) has depended on information relay from area 3b of S1 for activation (N20-P25) (Kaas, 2004). Notably, there is a distinction between the habituation response within S1 between the areas 3b and 1–2, which could mainly imply that N20 is a primary S1 response without any sensory adaptation response, whereas early-to-middle SEP components, such as P45, exhibit memory traces from secondary sensory areas (although they originate from S1) (Bradley et al., 2016). It is possible that the effect seen at the N33-P45 component comes from a superficial neuroanatomical perspective or from information being relayed from area 3b – to area 1/2 within S1. In sum, the effect on N20-P25 and N33-P45 early SEPs provides evidence that M1 homeostatic plasticity induction influenced S1 excitability, but not in the manner that was hypothesized.

Anodal tDCS stimulation to M1 induced lasting facilitation of S1 SEPs

Contrary to the hypothesis, the anodal tDCS homeostatic plasticity protocol over M1 resulted in lasting facilitation of N20-P25, N33-P45 complex, and P45 peak amplitude, with no indication of a homeostatic plasticity response in S1. The current findings are in line with an earlier study, where 10 mins of anodal sensorimotor tDCS caused a lasting increase in early parietal SEP components (P22-N33, P25-N33, N33-P40) (Matsunaga et al., 2004). Interestingly, 20 mins of anodal tDCS over M1 has also been shown to decrease N20-P25 amplitude and increase in MEPs amplitude (Vaseghi et al., 2015b). However, when anodal tDCS was applied to S1, they observed a facilitation of the N20-P25 amplitude (Vaseghi et al., 2015b). A likely contributing factor to this confounding evidence is the inter-individual anatomical variation (Li et al., 2015) since current flow simulations and human studies have reported that the intensity and distribution of the electric

field induced by tDCS is highly dependent on individual brain anatomy and conductivity of each tissue (Opitz et al., 2015). This suggests that the applied current strength at electrode placement is different than the current strength at the target site. Additionally, stimulation time differences between studies may also contribute to this confounding evidence. The above confirms the need for more neurophysiological studies exploring the effect of M1 anodal tDCS stimulation on S1 excitability.

Cathodal tDCS stimulation to M1 did not elicit significant changes to S1 excitability

The cathodal homeostatic plasticity induction protocol over M1 did not yield a significant homeostatic plasticity response, while a decrease for post-10 min in the N20-P25 component was found. For N20, P25, and N33, the type of tDCS showed a significant difference between anodal and cathodal stimulation. In line with the current findings, Matsunaga et al. (2004), found that N20-P25 remained in the range below baseline and a slight increase above baseline was seen for the N33-P40, after cathodal stimulation. In contrast, two studies found inhibition of early SEPs after cathodal tDCS (Dieckhöfer et al., 2006; Vaseghi et al., 2015a). The discrepancy in the observed effects between the latter studies (Matsunaga et al., 2004; Dieckhöfer et al., 2006; Vaseghi et al., 2015a) could most likely be due to differences in electrical field distribution due to the location and size of electrodes. Of note, anodal and cathodal stimulation do not always yield facilitation or inhibition, respectively, and this is particularly true for areas outside of the primary motor cortex (Jacobson et al., 2012), indicating that the cortical response to cathodal tDCS is not always dependent on polarity but also on the assessed cortical area (Matsunaga et al., 2004; Marshall et al., 2005; Sparing et al., 2008; Galea and Jayaram, 2009; Tanaka et al., 2009; Jacobson et al., 2012).

Primary motor cortex homeostatic plasticity induction did not yield a similar response in S1

The current findings did not support the hypothesis that M1 stimulation can elicit a homeostatic response in S1, as the changes in early- and middle-latency SEPs did not follow homeostatic regulation rules. Post-priming SEPs were not facilitated, but it is known that overt plasticity between the two blocks is not necessary to induce a homeostatic response (Karabanov et al., 2015). Moreover, early and middle-latency SEPs at and after Post-HP were facilitated which is contrary to the hypothesized reduction due to homeostatic regulation. One possibility is that M1 homeostatic plasticity induction did not cause a significant change in the somatosensory system. For M1 homeostatic plasticity induction, the electrodes used in this experiment were smaller (12 mm diameter, 1.131 cm^2 Ag/AgCl gel electrodes) than other homeostatic plasticity studies (Wittkopf et al., 2021b, 2021a) which commonly employ 5x7 cm, 35 cm^2 sponge electrodes (Wittkopf et al., 2021b, 2021a), which is important given that electrode size can change the tDCS effect on the underlying neural tissue (Caulfield and George, 2022). Based on the findings of the present study, it might be speculated that the impairment of M1 homeostatic plasticity seen in pain states (Thapa et al., 2018, 2021) may be unrelated to S1 activity. Additionally, it may be reasonable to state that to observe a homeostatic plasticity effect from S1 a more specific stimulation targeting S1 is needed (i.e., rather than diffusion effects of M1 tDCS). Notably, while M1 tDCS stimulation demonstrably affects S1 excitability (Matsunaga et al., 2004; Vaseghi et al., 2015a), this may not be the case for homeostatic regulation. This notion is, at least partially, supported by an earlier study where homeostatic plasticity was induced at S1, and a homeostatic response was evaluated based on SEPs (Bliem et al., 2008). Bliem et al. (Bliem et al., 2008), applied two different PAS protocols to induce either LTP- or LTD-like plasticity, followed by peripheral high-frequency stimulation (pHFS) of the median nerve. Observable decreases in the excitability of P25 and N20-P25 SEP components followed the rules of homeostatic plasticity regulation after two LTP-like stimulation protocols (Bliem et al., 2008). However, contrasting evidence is available where an homeostatic plasticity response in SEPs was not found after theta-burst stimulation (TBS) over S1, and both priming and homeostatic plasticity protocols with iTBS (intermittent TBS, facilitatory) yielded an increase in S1 excitability as reflected by N20-P25 SEPs (Jones et al., 2016). More studies are needed to understand the potential homeostatic plasticity manifestation in S1. A promising method to evaluate homeostatic responses on cortical regions outside the motor system is TMS-EEG (Cruciani et al., 2023), with which an increase in cortical excitability during and after 15 min of anodal tDCS has been demonstrated (Romero Lauro et al., 2014). On the other hand, cathodal tDCS of M1 reduced early TMS-evoked peaks, regionally, in a dose-dependent manner, and had widespread effects at a global scalp level (Mosayebi-Samani et al., 2023). Of interest, is that regional specific changes where specific to M1 tDCS and not prefrontal cortex tDCS (Mosayebi-Samani et al., 2023). Thus, using TMS-EEG to evaluate homeostatic responses would highlight the plausible regional or global nature of homeostatic plasticity, by simultaneously studying the response of multiple brain regions. In sum, there is available evidence on the priming effect of S1 anodal and cathodal stimulation on SEPs (Matsunaga et al., 2004; Vaseghi et al., 2015a), but it is still unknown if S1 anodal or cathodal homeostatic plasticity protocols can elicit an S1 homeostatic response but warrants further investigation.

Limitations

This study used a reliable methodology for inducing homeostatic responses in the corticomotor system (Thapa and Schabrun, 2018), but the effect is variable among individuals. Thus, while several studies using this methodology have reported M1 homeostatic responses (Thapa and Schabrun, 2018; Thapa et al., 2018, 2021; Wittkopf et al., 2021b), the most important limitation of this study is that measures of corticomotor excitability (i.e., MEPs) were not recorded, and M1 homeostatic plasticity can therefore only be assumed. A future study would need to replicate these findings with an additional session where MEPs are recorded in the same subjects and M1 homeostatic plasticity is confirmed. A second limitation concerns the location for M1, which was selected at electrode C3 (based on the 10–20 international system) for all subjects without any neuronavigational techniques or relation to MEP amplitude. Although M1 location can vary among subjects (Kim et al., 2023), evidence-based guidelines for most experimental and clinical trial studies, state that M1 has been usually defined as the location of C3/C4 electrode in the international 10–20 system (Lefaucheur et al., 2017), and not as the motor hotspot of the hand (i.e., abductor digiti minimi MEPs). Additionally, using the EEG 10–20 system as a standard reference may reduce the variability in individual measurements and has proven to be congruent with high-resolution MRI anatomical landmarks (Herwig et al., 2003). Finally, while anodal and cathodal are two contrasting conditions, a sham condition is still needed to understand the effect of the experiment design and time in the SEPs (e.g., habituation). Habituation is a normal physiological mechanism observed in early SEPs of healthy volunteers (Ozkul and Uckardes, 2002; Coppola et al., 2012). This is in part justified as each stimulus in this study was given to avoid habituation (i.e., with a varying delay), which was not done in the previous studies (Ozkul and Uckardes, 2002; Coppola et al., 2012). The lack of a sham condition may also be partly justified by earlier studies where sham tDCS has not significantly modified SEPs (Kirimoto et al., 2011; Sehm et al., 2013; Vaseghi et al., 2015b, 2015a).

Conclusion

This study is the first to evaluate whether a reliably tested M1 homeostatic plasticity induction protocol could induce changes in S1 excitability and whether these changes would yield a homeostatic plasticity response. Anodal M1 homeostatic plasticity induction facilitated early and middle-latency SEPs up to 20 min post-induction, without any evidence of S1 homeostatic plasticity. These results suggest that M1 homeostatic plasticity directly regulates SEPs but without a homeostatic response. Further research is needed to determine if a homeostatic response can be detected in the sensory system using a different methodology.

Declaration of competing interest

The authors declare that they have no known competing financial interests or personal relationships that could have appeared to influence the work reported in this paper.

CRediT authorship contribution statement

Daniela M. Zolezzi: Writing – original draft, Data curation, Formal analysis, Investigation, Methodology, Software, Writing – review & editing. **Dennis B. Larsen:** Conceptualization, Methodology, Supervision, Validation, Visualization, Writing – review & editing. **Anna M. Zamorano:** Data curation, Supervision, Writing – review & editing. **Thomas Graven-Nielsen:** Conceptualization, Funding acquisition, Investigation, Project administration, Resources, Supervision, Validation, Visualization, Writing – review & editing.

Acknowledgments

The Center for Neuroplasticity and Pain (CNAP) is supported by the Danish National Research Foundation (DNRF121).

Appendix A. Supplementary material

Supplementary material to this article can be found online at https://doi.org/10.1016/j.neuroscience.2024.05.001.

References

Allison, T., Mccarthy, G., Wood, C.C., Darcey, T.M., Spencer, D.D., Williamson, P.D., 1989a. Human cortical potentials evoked by stimulation of the median nerve. I. Cytoarchitectonic areas generating short-latency activity. J. Neurophysiol. 62.

Allison, T., Mccarthy, G., Wood, C.C., Williamson, P.D., Spencer, D.D., 1989b. Human cortical potentials evoked by stimulation of the median nerve. II. Cytoarchitectonic areas generating long-latency activity. J. Neurophysiol. 62.

Allison, T., Mccarthy, G., Wood, C.C., Jones, S.J., 1991. Potentials evoked in human and monkey cerebral cortex by stimulation of the median nerve. A review of scalp and intracranial recordings. Brain 114 (Pt 6), 2465–2503 [Accessed July 22, 2022] https://pubmed.ncbi.nlm.nih.gov/1782527/.

Bienenstock, E., Cooper, L., Munro, P., 1982. Theory for the development of neuron selectivity: orientation specificity and binocular interaction in visual cortex. J. Neurosci. 2, 32. /pmc/articles/PMC6564292/?report=abstract [Accessed October 29, 2021].

Bliem, B., Müller-Dahlhaus, J.F.M., Dinse, H.R., Ziemann, U., 2008. Homeostatic metaplasticity in the human somatosensory cortex. J. Cogn. Neurosci. 20, 1517–1528.

Bradley, C., Joyce, N., Garcia-Larrea, L., 2016. Adaptation in human somatosensory cortex as a model of sensory memory construction: a study using high-density EEG. Brain Struct. Funct. 221, 421–431. https://doi.org/10.1007/s00429-014-0915-5 [Accessed May 11, 2023].

Caulfield, K.A., George, M.S., 2022. Optimized APPS-tDCS electrode position, size, and distance doubles the on-target stimulation magnitude in 3000 electric field models. Sci. Rep. 12, 20116. https://doi.org/10.1038/s41598-022-24618-3 [Accessed May 26, 2023].

Chang, C.Y., Hsu, S.H., Pion-Tonachini, L., Jung, T.P., 2020. Evaluation of artifact subspace reconstruction for automatic artifact components removal in multi-channel EEG recordings [Accessed June 2, 2023] IEEE Trans. Biomed. Eng. 67, 1114–1121 https://pubmed.ncbi.nlm.nih.gov/31329105/.

Coppola, G., De Pasqua, V., Pierelli, F., Schoenen, J., 2012. Effects of repetitive transcranial magnetic stimulation on somatosensory evoked potentials and high frequency oscillations in migraine. Cephalalgia 32, 700–709.

Cruccu, G., Aminoff, M.J., Curio, G., Guerit, J.M., Kakigi, R., Mauguiere, F., Rossini, P. M., Treede, R.D., Garcia-Larrea, L., 2008. Recommendations for the clinical use of somatosensory-evoked potentials. Clin. Neurophysiol. 119, 1705–1719.

Cruciani, A., Mancuso, M., Sveva, V., Maccarrone, D., Todisco, A., Motolese, F., Santoro, F., Pilato, F., Spampinato, D.A., Rocchi, L., Di Lazzaro, V., Capone, F., 2023. Using TMS-EEG to assess the effects of neuromodulation techniques: a narrative review. Front. Hum. Neurosci. 17.

Cruciani, A., Pellegrino, G., Todisco, A., Motolese, F., Sferruzzi, M., Norata, D., Santoro, F., Musumeci, G., Rossi, M., Pilato, F., Di Lazzaro, V., Capone, F., 2024. High-frequency transcranial alternating current stimulation matching individual frequency of somatosensory evoked high-frequency oscillations can modulate the somatosensory system through thalamocortical pathway. Cereb. Cortex 34.

De Martino, E., Petrini, L., Schabrun, S., Graven-Nielsen, T., 2018. Cortical somatosensory excitability is modulated in response to several days of muscle soreness. J. Pain 19, 1296–1307.

Desmedt, J.E., Huy Nguyen, T., Bourguet, M., 1987. Bit-mapped color imaging of human evoked potentials with reference to the N20, P22, P27 and N30 somatosensory responses. Electroencephalogr. Clin. Neurophysiol./Evoked Potentials 68, 1–19.

Dieckhöfer, A., Waberski, T.D., Nitsche, M., Paulus, W., Buchner, H., Gobbelé, R., 2006. Transcranial direct current stimulation applied over the somatosensory cortex – Differential effect on low and high frequency SEPs. Clin. Neurophysiol. 117, 2221–2227.

Enomoto, H., Ugawa, Y., Hanajima, R., Yuasa, K., Mochizuki, H., Terao, Y., Shiio, Y., Furubayashi, T., Iwata, N.K., Kanazawa, I., 2001. Decreased sensory cortical excitability after 1 Hz rTMS over the ipsilateral primary motor cortex. Clin. Neurophysiol. 112, 2154–2158.

Fabbrini, A., Guerra, A., Giangrosso, M., Manzo, N., Leodori, G., Pasqualetti, P., Conte, A., Di Lazzaro, V., Berardelli, A., 2022. Transcranial alternating current stimulation modulates cortical processing of somatosensory information in a frequency- and time-specific manner. Neuroimage 254, 119119.

Frot, M., Magnin, M., Mauguière, F., Garcia-Larrea, L., 2013. Cortical representation of pain in primary sensory-motor areas (S1/M1)—a study using intracortical recordings in humans. Hum. Brain Mapp. 34, 2655–2668. https://doi.org/10.1002/hbm.22097 [Accessed May 10, 2023].

G, T., 2011. Too many cooks? Intrinsic and synaptic homeostatic mechanisms in cortical circuit refinement. Annu. Rev. Neurosci. 34, 89–103 [Accessed October 29, 2021] https://pubmed.ncbi.nlm.nih.gov/21438687/.

Galea, J., Jayaram, G., 2009. Modulation of cerebellar excitability by polarity-specific noninvasive direct current stimulation. Soc. Neurosci. [Accessed April 26, 2023] https://www.jneurosci.org/content/29/28/9115.short.

Garraghty, P.E., Florence, S.L., Kaas, J.H., 1990. Ablations of areas 3a and 3b of monkey somatosensory cortex abolish cutaneous responsivity in area 1. Brain Res 528, 165–169 [Accessed May 16, 2023] https://pubmed.ncbi.nlm.nih.gov/2245335/.

Hashimoto, I., Mashiko, T., Imada, T., 1996. Somatic evoked high-frequency magnetic oscillations reflect activity of inhibitory interneurons in the human somatosensory cortex. Electroencephalogr. Clin. Neurophysiol./Evoked Potent. Sect. 100, 189–203.

Herwig, U., Satrapi, P., Schönfeldt-Lecuona, C., 2003. Using the international 10–20 EEG system for positioning of transcranial magnetic stimulation [Accessed June 1, 2023] Brain Topogr. 16, 95–99 https://pubmed.ncbi.nlm.nih.gov/14977202/.

Inui, K., Wang, X., Tamura, Y., Kaneoke, Y., Kakigi, R., 2004. Serial processing in the human somatosensory system. Cereb. Cortex 14, 851–857 [Accessed May 15, 2023] https://pubmed.ncbi.nlm.nih.gov/15054058/.

Jacobson, L., Koslowsky, M., Lavidor, M., 2012. TDCS polarity effects in motor and cognitive domains: A meta-analytical review. Exp. Brain Res. 216, 1–10. https://doi.org/10.1007/s00221-011-2891-9 [Accessed April 26, 2023].

Jones, E.G., Coulter, J.D., Hendry, S.H.C., 1978. Intracortical connectivity of architectonic fields in the somatic sensory, motor and parietal cortex of monkeys. J. Comp. Neurol. 181, 291–347.

Jones, C.B., Lulic, T., Bailey, A.Z., Mackenzie, T.N., Mi, Y.Q., Tommerdahl, M., Nelson, A.J., 2016. Metaplasticity in human primary somatosensory cortex: effects on physiology and tactile perception. 101152/jn006302015 115, 2681–2691. https://doi.org/10.1152/jn.00630.2015 [Accessed October 18, 2021].

Kaas, J.H., 2004. Evolution of somatosensory and motor cortex in primates. Anat. Rec. A Discov. Mol. Cell Evol. Biol. 281A, 1148–1156. https://doi.org/10.1002/ar.a.20120 [Accessed May 16, 2023].

Kang, J.-S., Terranova, C., Hilker, R., Quartarone, A., Ziemann, U., 2011. Deficient homeostatic regulation of practice-dependent plasticity in Writer's cramp. Cereb. Cortex 21, 1203–1212.

Karabanov, A., Ziemann, U., Hamada, M., George, M.S., Quartarone, A., Classen, J., Massimini, M., Rothwell, J., Siebner, H.R., 2015. Consensus Paper: Probing homeostatic plasticity of human cortex with non-invasive transcranial brain stimulation. Brain Stimul. 8, 442–454.

Keel, J.C., Smith, M.J., Wassermann, E.M., 2001. A safety screening questionnaire for transcranial magnetic stimulation. Clin. Neurophysiol. 112, 720.

Kim, H., Wright, D.L., Rhee, J., Kim, T., 2023. C3 in the 10–20 system may not be the best target for the motor hand area. Brain Res. 1807, 148311.

Kirimoto, H., Ogata, K., Onishi, H., Oyama, M., Goto, Y., Tobimatsu, S., 2011. Transcranial direct current stimulation over the motor association cortex induces plastic changes in ipsilateral primary motor and somatosensory cortices. Clin. Neurophysiol. 122, 777–783.

Knecht, S., Kunesch, E., Schnitzler, A., 1996. Parallel and serial processing of haptic information in man: Effects of parietal lesions on sensorimotor hand function. Neuropsychologia 34, 669–687.

Lefaucheur, J.P. et al, 2017. Evidence-based guidelines on the therapeutic use of transcranial direct current stimulation (tDCS). Clin. Neurophysiol. 128, 56–92.
Li, L.M., Uehara, K., Hanakawa, T., 2015. The contribution of interindividual factors to variability of response in transcranial direct current stimulation studies. Front. Cell Neurosci. 9, 141424.
Marshall, L., Mölle, M., Siebner, H.R., Born, J., 2005. Bifrontal transcranial direct current stimulation slows reaction time in a working memory task. BMC Neurosci. 6, 23.
Matsunaga, K., Nitsche, M.A., Tsuji, S., Rothwell, J.C., 2004. Effect of transcranial DC sensorimotor cortex stimulation on somatosensory evoked potentials in humans. Clin. Neurophysiol. 115, 456–460.
Mayka, M.A., Corcos, D.M., Leurgans, S.E., Vaillancourt, D.E., 2006. Three-dimensional locations and boundaries of motor and premotor cortices as defined by functional brain imaging: A meta-analysis. Neuroimage 31, 1453–1474.
Mosayebi-Samani, M., Agboada, D., Mutanen, T.P., Haueisen, J., Kuo, M.-F., Nitsche, M. A., 2023. Transferability of cathodal tDCS effects from the primary motor to the prefrontal cortex: A multimodal TMS-EEG study. Brain Stimul. 16, 515–539.
Nitsche, M.A., Paulus, W., 2000. Excitability changes induced in the human motor cortex by weak transcranial direct current stimulation. J. Physiol. 527, 633–639.
Opitz, A., Paulus, W., Will, S., Antunes, A., Thielscher, A., 2015. Determinants of the electric field during transcranial direct current stimulation. Neuroimage 109, 140–150.
Ozkul, Y., Uckardes, A., 2002. Median nerve somatosensory evoked potentials in migraine. Eur. J. Neurol. 9, 227–232.
Pion-Tonachini, L., Kreutz-Delgado, K., Makeig, S., 2019. ICLabel: An automated electroencephalographic independent component classifier, dataset, and website. Neuroimage.
Poreisz, C., Boros, K., Antal, A., Paulus, W., 2007. Safety aspects of transcranial direct current stimulation concerning healthy subjects and patients. Brain Res. Bull. 72, 208–214 https://www.embase.com/search/results?subaction=viewrecord&id=L46602748&from=export.
Quartarone, A., Rizzo, V., Bagnato, S., Morgante, F., Sant'Angelo, A., Romano, M., Crupi, D., Girlanda, P., Rothwell, J.C., Siebner, H.R., 2005. Homeostatic-like plasticity of the primary motor hand area is impaired in focal hand dystonia. Brain 128, 1943–1950.
Randolph, M., Semmes, J., 1974. Behavioral consequences of selective subtotal ablations in the postcentral gyrus ofMacaca mulatta. Brain Res. 70, 55–70.
Rezaei, A., Lahtinen, J., Neugebauer, F., Antonakakis, M., Piastra, M.C., Koulouri, A., Wolters, C.H., Pursiainen, S., 2021. Reconstructing subcortical and cortical somatosensory activity via the RAMUS inverse source analysis technique using median nerve SEP data. Neuroimage 245, 118726.
Rocco-Donovan, M., Ramos, R.L., Giraldo, S., Brumberg, J.C., 2011. Characteristics of synaptic connections between rodent primary somatosensory and motor cortices. Somatosens Mot Res 28, 63–72.
Romero Lauro, L.J., Rosanova, M., Mattavelli, G., Convento, S., Pisoni, A., Opitz, A., Bolognini, N., Vallar, G., 2014. TDCS increases cortical excitability: Direct evidence from TMS–EEG. Cortex 58, 99–111.
Saturnino, G.B., Puonti, O., Nielsen, J.D., Antonenko, D., Madsen, K.H., Thielscher, A., 2019. SimNIBS 2.1: A comprehensive pipeline for individualized electric field modelling for transcranial brain stimulation. In: Brain and Human Body Modeling. Springer International Publishing, Cham, pp. 3–25.
Schabrun, S.M., Jones, E., Kloster, J., Hodges, P.W., 2013. Temporal association between changes in primary sensory cortex and corticomotor output during muscle pain. Neuroscience 235, 159–164.
Sehm, B., Hoff, M., Gundlach, C., Taubert, M., Conde, V., Villringer, A., Ragert, P., 2013. A novel ring electrode setup for the recording of somatosensory evoked potentials during transcranial direct current stimulation (tDCS). J. Neurosci. Methods 212, 234–236.
Siebner, H., Rothwell, J., 2003. Transcranial magnetic stimulation: new insights into representational cortical plasticity. Exp. Brain Res. 148, 1–16. https://doi.org/10.1007/s00221-002-1234-2 [Accessed October 15, 2021].
Sparing, R., Dafotakis, M., Meister, I.G., Thirugnanasambandam, N., Fink, G.R., 2008. Enhancing language performance with non-invasive brain stimulation—a transcranial direct current stimulation study in healthy humans. Neuropsychologia 46, 261–268.
Tanaka, S., Hanakawa, T., Honda, M., Watanabe, K., 2009. Enhancement of pinch force in the lower leg by anodal transcranial direct current stimulation [Accessed April 26, 2023] Exp. Brain Res. 196, 459–465 https://www.ncbi.nlm.nih.gov/pmc/articles/pmid/19479243/?tool=EBI.
Thapa, T., 2018. Schabrun SM (2018) Test-retest reliability of homeostatic plasticity in the human primary motor cortex. Neural Plast..
Thapa, T., Graven-Nielsen, T., Chipchase, L.S., Schabrun, S.M., 2018. Disruption of cortical synaptic homeostasis in individuals with chronic low back pain. Clin. Neurophysiol. 129, 1090–1096.
Thapa, T., Graven-Nielsen, T., Schabrun, S.M., 2021. Aberrant plasticity in musculoskeletal pain: a failure of homeostatic control? Exp. Brain Res. 239, 1317–1326. https://doi.org/10.1007/s00221-021-06062-3.
Tomberg, C., Desmedt, J.E., Ozaki, I., 1991. Right or left ear reference changes the voltage of frontal and parietal somatosensory evoked potentials [Accessed June 2, 2023] Electroencephalogr. Clin. Neurophysiol. 80, 504–512 https://pubmed.ncbi.nlm.nih.gov/1720726/.
Turrigiano, G., 2012. Homeostatic synaptic plasticity: Local and global mechanisms for stabilizing neuronal function. Cold Spring Harb. Perspect. Biol. 4.
Turrigiano, G.G., Nelson, S.B., 2004. Homeostatic plasticity in the developing nervous system. Nat. Rev. Neurosci. 5, 97–107 [Accessed October 18, 2021] https://www.nature.com/articles/nrn1327.
Valeriani, M., Barba, C., Le Pera, D., Restuccia, D., Colicchio, G., Tonali, P., Gagliardo, O., Treede, R.D., 2004. Different neuronal contribution to N20 somatosensory evoked potential and to CO_2 laser evoked potentials: an intracerebral recording study. Clin. Neurophysiol. 115, 211–216.
Vaseghi, B., Zoghi, M., Jaberzadeh, S., 2015a. Differential effects of cathodal transcranial direct current stimulation of prefrontal, motor and somatosensory cortices on cortical excitability and pain perception - a double-blind randomised sham-controlled study. Eur. J. Neurosci. 42, 2426–2437.
Vaseghi, B., Zoghi, M., Jaberzadeh, S., 2015b. How does anodal transcranial direct current stimulation of the pain neuromatrix affect brain excitability and pain perception? A randomised, double-blind, sham-control study. Plos One 10, e0118340.
Wittkopf, P.G., Larsen, D.B., Graven-Nielsen, T., 2021a. Protocols for inducing homeostatic plasticity reflected in the corticospinal excitability in healthy human participants: A systematic review and meta-analysis. Eur. J. Neurosci. 54, 5444–5461.
Wittkopf, P.G., Larsen, D.B., Gregoret, L., Graven-Nielsen, T., 2021b. Prolonged corticomotor homeostatic plasticity – Effects of different protocols and their reliability. Brain Stimul. 14, 327–329. https://doi.org/10.1016/j.brs.2021.01.017.
Wittkopf, P.G., Larsen, D.B., Gregoret, L., Graven-Nielsen, T., 2021c. Prolonged corticomotor homeostatic plasticity – Effects of different protocols and their reliability. Brain Stimul. 14, 327–329.
Wittkopf, P.G., Larsen, D.B., Gregoret, L., Graven-Nielsen, T., 2023. Disrupted cortical homeostatic plasticity due to prolonged capsaicin-induced pain. Neuroscience.
Ziemann, U., Paulus, W., Nitsche, M.A., Pascual-Leone, A., Byblow, W.D., Berardelli, A., Siebner, H.R., Classen, J., Cohen, L.G., Rothwell, J.C., 2008. Consensus: Motor cortex plasticity protocols. Brain Stimul. 1, 164–182.